RESEARCH ARTICLE

B-1 cell-mediated modulation of M1 macrophage profile ameliorates microbicidal functions and disrupt the evasion mechanisms of *Encephalitozoon cuniculi*

Adriano Pereira[1,2☯], Anuska Marcelino Alvares-Saraiva[1,3,4☯], Fabiana Toshie de Camargo Konno[1], Diva Denelle Spadacci-Morena[4], Elizabeth Cristina Perez[1], Mario Mariano[1], Maria Anete Lallo[1,2]*

1 Programa de Patologia Ambiental e Experimental, Universidade Paulista, Rua José Maria Whitaker, São Paulo, SP, Brasil, **2** Curso de Biomedicina, Centro Universitário São Camilo, São Paulo, SP, Brazil, **3** Programa de Pós-Graduação Interdisciplinar em Ciências da Saúde, Universidade Cruzeiro do Sul, Rua Galvão Bueno, São Paulo, SP, Brazil, **4** Laboratório de Fisiopatologia, Instituto Butantan, São Paulo, SP, Brasil

☯ These authors contributed equally to this work.
* anetelallo@hotmail.com, maria.lallo@docente.unip.br

Abstract

Here, we have investigated the possible effect of B-1 cells on the activity of peritoneal macrophages in *E. cuniculi* infection. In the presence of B-1 cells, peritoneal macrophages had an M1 profile with showed increased phagocytic capacity and index, associated with the intense microbicidal activity and a higher percentage of apoptotic death. The absence of B-1 cells was associated with a predominance of the M2 macrophages, reduced phagocytic capacity and index and microbicidal activity, increased pro-inflammatory and anti-inflammatory cytokines production, and higher percentual of necrosis death. In addition, in the M2 macrophages, spore of phagocytic *E. cuniculi* with polar tubular extrusion was observed, which is an important mechanism of evasion of the immune response. The results showed the importance of B-1 cells in the modulation of macrophage function against *E. cuniculi* infection, increasing microbicidal activity, and reducing the fungal mechanisms involved in the evasion of the immune response.

Author summary

The adaptive immune response plays a key role against *Encephalitozoon cuniculi*, an opportunistic fungus for T cells immunodeficient patients. The role of B cells and antibody play in natural resistance to *Encephalitozoon cuniculi* remains unknown. Previously, we demonstrated that B-1 deficient mice (XID), an important component of innate immunity, were more susceptible to encephalitozoonosis, despite the increase in the number of CD4^{+} and CD8^{+} T lymphocytes. Here we observed that the absence of B-1 cells was associated with a larger population of M2 macrophages, a balance between anti-inflammatory and pro-inflammatory cytokines profile, which had lower microbicidal activity

against *E. cuniculi* infection. However, in the presence of B-1 cells, peritoneal macrophages had a M1 profile with showed increased microbicidal activity and a higher percentage of apoptotic death.

Introduction

Microsporidia are obligate intracellular spore-forming microorganisms that can infect a wide range of vertebrate and invertebrate species. These fungi have been recognized as human pathogens and are particularly harmful to immunodeficient patients infected with HIV. Since then, interest among researchers of *in vitro* culture techniques has increased, with more people studying their biology and immune response against them [1].

Encephalitozoon cuniculi is one of the most common microsporidian species, in humans or animals. It is considered to be an emerging zoonotic and opportunistic pathogen in immuno-compromised as well as immunocompetent individuals [2]. Spores of *E. cuniculi* can survive in macrophages, spread throughout the host, and cause lesions in organs of the urinary, digestive, respiratory, and nervous systems [3].

The adaptive immune response is critical for the elimination of *E. cuniculi*, but the innate immune response forms the first line of defense against these pathogens. The infection by *E. cuniculi* induces CD8+ cytotoxic T lymphocyte (CTL) response, which lyses the infected cells by perforin-dependent mechanisms [1]. Although antibody response during *E. cuniculi* infection has been recorded, it is clearly not sufficient to prevent mortality or cure the infection, making cell-mediated immunity critical for the survival of host infected by *E. cuniculi* [4]. The survival and replication of certain species of microsporidia within macrophages may be associated with the absence of phagosome-lysosome fusion [5]. Internalized microsporidium spores are normally destroyed within macrophages by the toxic activity of reactive oxygen and nitrogen species produced by the respiratory burst, and cytokines released by macrophages may be important in the protection against microsporidia [6].

B-1 cells are a subtype of B cells that account for 35%-70% of the B cells in the peritoneal cavity of mice [7]. They differ from B-2 cells in the expression of surface markers and function [8]. B-1 cells act as antigen-presenting cells, phagocytes, expressing myeloid (CD11b) and lymphoid markers (CD45/B220, CD5, CD19 and IgM), but not CD23, unlike B-2 cells [9]. The main function of B-1 cells in the innate immune system is the spontaneous secretion of natural antibodies, thereby maintaining immunoglobulin levels in the body without any stimulus or immunization [10]. In addition, B-1 cells also spontaneously secrete IL-10, while GM-CSF and IL-3 are secreted after lipopolysaccharide stimulation [10]. B-1 cells also regulate acute and chronic inflammatory diseases through the production of several immunomodulatory molecules, such as interleukin-10 (IL-10), adenosine, granulocyte-macrophage colony-stimulating factor (GM-CSF), IL-13, and IL-35, in the presence or absence of stimulus [11].

The possible role of B-1 cells in the dynamics of the inflammatory process of various etiologies is unknown and researchers have demonstrated the role of these cells in the functional regulation of macrophages. Also, B-1 cells are able to differentiate into phagocytes (B-1CDP), characterized by the expression of F4/80 and increased phagocytic activity [12,13]. Furthermore, Popi *et al.* [14] demonstrated that BALB/c mice were more susceptible to *Paracocci-dioides brasiliensis* infection compared to XID (B-1 cell deficient) mice and attributed the down-regulation of macrophage function to IL-10 secreted by B-1 cells.

In recent studies from our group, we demonstrated that B-1 cell deficient XID mice were more susceptible to experimental encephalitozoonosis than BALB/c mice, evidenced

histologically with more prominent inflammatory lesions and fungal burden [15,16]. Although the mechanism of action of B-1 cells in the resistance of BALB/c mice to encephalitozoonosis is not fully understood, a significant increase in the population of peritoneal macrophages was reported in BALB/c mice infected with *E. cuniculi* [15]. We hypothesized that B-1 cells from the peritoneal cavity (PerC) could differentiate in infected animals into B-1 cell-derived phagocytes (B-1 CDP), which could then promote the phagocytosis of *E. cuniculi* spores and also influence the macrophage function in this context. Herein, we tested this hypothesis using the ultrastructure and phenotypic analysis of adherent peritoneal cells (APerC) to evaluate their *in vitro* behavior in BALB/c and B-1 cell-deficient XID mice against the fungus *E. cuniculi*. The presence of B-1 cells facilitated the phagocytic and microbicidal activity and increased apoptosis in the APerC cultures. These cells were associated with the presence of M1 macrophages with increased proinflammatory cytokine production. Electron micrographs showed an intimate physical relationship between B-1 cells and macrophages, indicating communication and modulation of activity, demonstrating that the presence of B-1 cells drives the behavior of macrophages and consequently the innate immune response in encephalitozoonosis.

Results

B-1 cells increase macrophage activity in *E. cuniculi* infection

To assess the influence of B-1 cells on the activity of macrophages in *E. cuniculi* infection, APerC obtained from PerC of B-1 cell-containing BALB/c and B-1 cell-deficient XID mice were co-infected with *E. cuniculi* for ultrastructural analyses at 1, 48, and 144 h. The phagocytosis of spores occurred in cell cultures of both BALB/c and XID APerC groups, characterized by projections of the cellular membrane of macrophages near or around the spores (Fig 1A and 1B), and remained within phagosome vacuoles that were dispersed throughout the cytoplasm. XID macrophages showed large numbers of vacuoles in the cytoplasm and several membrane projections (pseudopods), indicating widespread and strong phagocytic activity (Fig 1A).

Intact and degenerating internalized spores surrounded by a vacuolar membrane, which is a typical phagosome vacuole, were observed (Fig 1C). Under normal circumstances, the interaction of phagosomes with each other and with other organelles is tightly regulated, and it is well documented that phagosomes containing inert particles are not subjected to homotypic fusion [17]. The important finding of this study is the formation of megasomes by the fusion of homotypic phagosomes containing a single *E. cuniculi* spore (Fig 1D). Therefore, the ability of *E. cuniculi* to induce the fusion of phagosomes resembles that of *Helicobacter pylori* [18] and *Chlamydia trachomatis* [19].

In AperC cultures of both BALB/c and XID mice, the microbicidal activity was identified by the presence of a large amount of amorphous and electron-dense material either inside the phagocytic vacuoles and megasome in the cytoplasm of macrophages or undergoing exocytosis (Fig 1B and 1D). The same findings were seen at 48 h (Fig 2A and 2D) with an increase in the ratio of degenerated spores, and at 144 h with only a few intact spores inside the phagocytic cells in case of XID AperC (S1A and S1B Fig). Myelin figures indicating spore degeneration were recorded (Fig 2B). Another important finding was the presence of degenerating macrophages (Fig 2D). At 144 h, the APerC of BALB/c showed an absence of macrophages and mature spores of *E. cuniculi* outside the cells (S1C and S1D Fig) and degenerated lymphocytes (S1D Fig). The intracellular proliferative stages of *E. cuniculi* (meronts, sporonts, or sporoblast) were not observed.

The B-1 cells were identified in BALB/c APerC by their ultrastructural morphological characteristics such as a lobed nucleus with bridges of the nuclear membrane joining the lobules and a well-developed endoplasmic reticulum with few mitochondria [20] (Fig 2E). We also
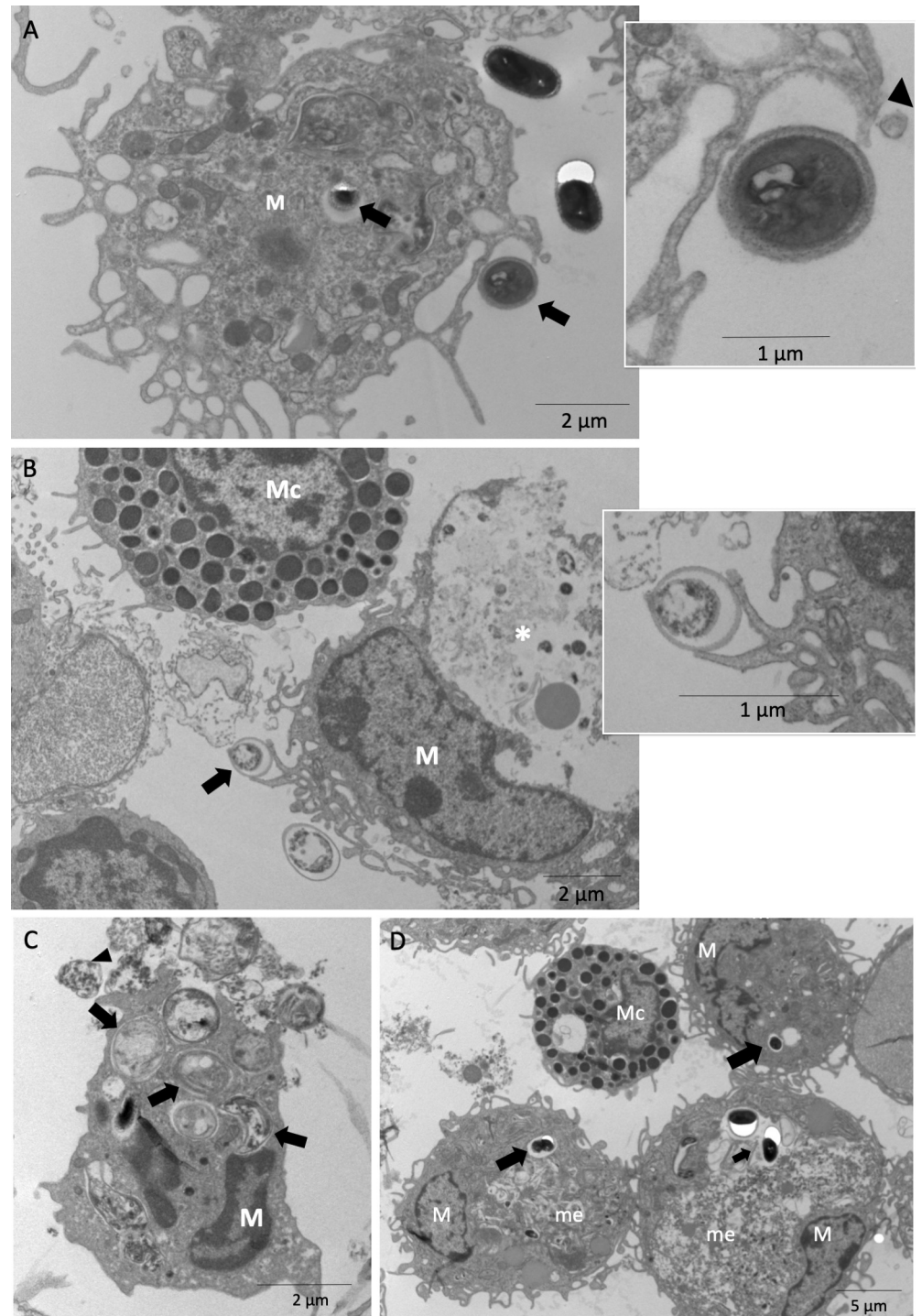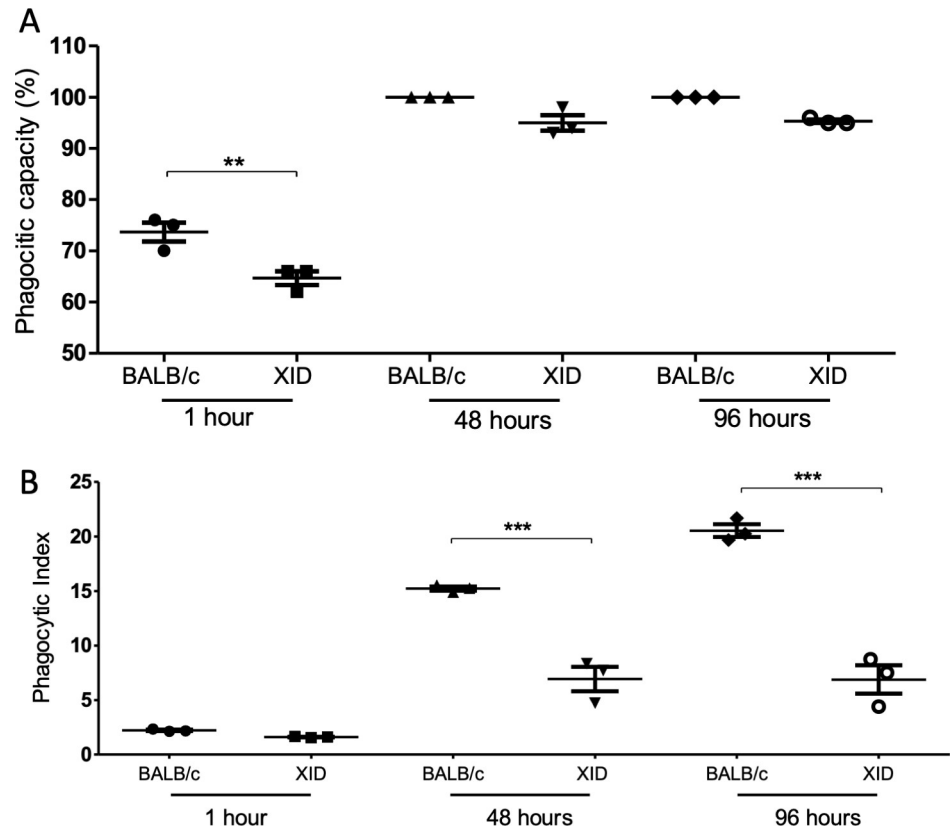
Fig 1. Phagocytic activity of BALB/c and XID APerC after 1 h of infection with *E. cuniculi* spores by ultramicrography. (A and insert) Projections of the cellular membrane (head arrows) of macrophages near or involving the spores (arrow) of *E. cuniculi* in XID APerC. (B and insert) Projections of the cellular membrane of macrophages involving *E. cuniculi* spore (arrow) of in BALB/c APerC and amorphous material (*) inside phagosome vacuole. Note the presence of mast cell. (C) Homotypic phagosomes vacuoles with *E. cuniculi* spores inside (arrow) and amorphous material exocytosed (head arrow) in BALB/c APerC macrophages. (D) Homotypic phagosomes vacuoles with intact spores (arrow) and megasome (me) with amorphous material inside in the macrophages (M) from XID APerC. Note mast cells (Mc) in contact with macrophages.
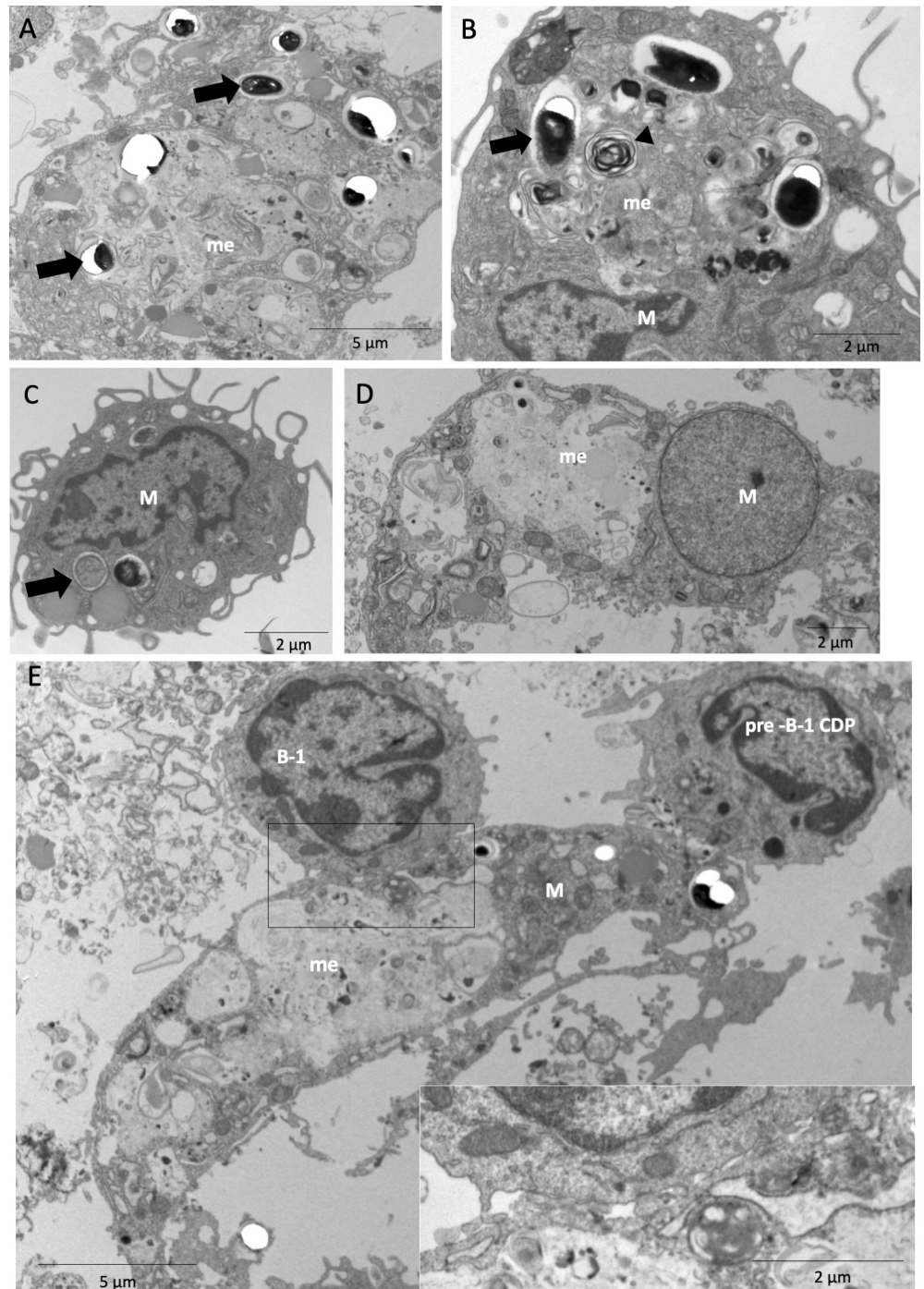
Fig 2. Phagocytic activity of BALB/c and XID APerC after 48 hours of infection with *E. cuniculi* spores. (A) Megasome (me) with amorphous and electron dense material and *E. cuniculi* spores (arrow) inside. Ultramicrography of macrophages from APerC BALB/c. (B) Megasome with amorphous and electrodense material, myelin figure (head arrow) and spores (arrow) in XID APerC by ultramicrography. (C) Homotypic phagosomes vacuoles in macrophages from APerC BALB/c by ultramicrography. (D) Degraded macrophage (M) containing amorphous material and involving spore of *E. cuniculi* in megasome (me) in XID APerC, by ultramicrography. (E) B-1 cells (B-1) and pre-B-1 CDP interaction with macrophage with a large megasome (me). Insert: Note the close relationship between macrophage membranes and B-1 cell.

Fig 3. Phagocytic activity of BALB/c and XID mice adherent peritoneal cells infected with _E. cuniculi_. The phagocytic capacity and phagocytic index were obtained from adherent peritoneal cells infected with _E. cuniculi_ after 1, 48, and 96 h. Data are represented as mean ± SEM ($^*P < 0.05$, $^{**}P < 0.01$, One way ANOVA with Tukey post-test).

observed the presence of cytoplasmic projections of pre-B-1 CDP cells and B-1 lymphocytes adhered to or near extracellular _E. cuniculi_ spores in BALB/c APerC (Fig 2E and insert). Inter-cellular communication involving other lymphocytes and mast cells and macrophages in BALB/c (Fig 1B) and XID APerC (Fig 1D).

Using Calcofluor stain, we observed increased phagocytic capacity and index in BALB/c APerC compared to XID APerC (Fig 3), suggesting the involvement of B-1 cells in the increase in phagocytic activity. After 1 h, large numbers of preserved spores were observed within the macrophages from BALB/c and XID, but after 48 h, there were fewer intact spores within the phagocytic vacuoles from BALB/c APerC, while the spores remained preserved in XID APerC.

Absence of B-1 cells reduces death by apoptosis but increases necrosis in _E. cuniculi_ infected APerC

As the ultrastructural analysis revealed that the BALB/c APerC phagocytes were no longer via-ble after 144 h, we evaluated the level of apoptosis and necrosis after 48 and 96 h for all experi-mental groups in order to examine the possible influence of _E. cuniculi_ in the process of cell death (Fig 4). Given the abundance of cell death accompanying intracellular infection, two possibilities have been described as evasion mechanisms: 1) the pathogen can be destroyed along with the engulfed apoptotic cell (host antimicrobial activity) or 2) the pathogen can use the process of efferocytosis to disperse into new cellular hosts ("Trojan Horse" model) [21]. About 50–60% of cell death was observed in BALB/c AperC, which was higher than that in
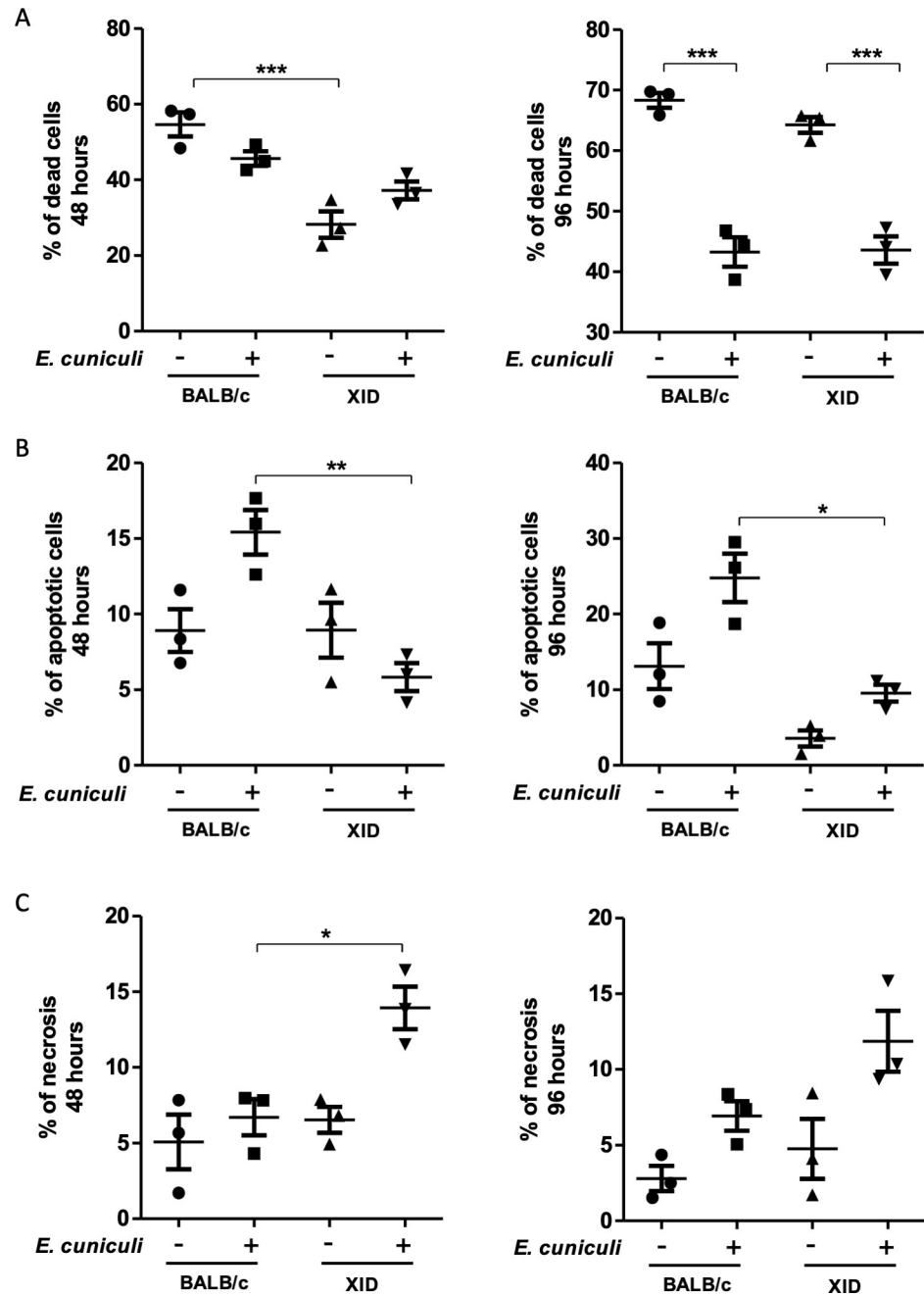
Fig 4. Necrosis and apoptosis of BALB/c and XID APerC cultures at 48 and 96 h. Percentual of: (A) death cells. (B) apoptotic cells. (C) necrotic cells. The data are presented as mean ± SEM (*$P < 0.05$, ** $P < 0.01$, *** $P < 0.001$, One way ANOVA with Tukey post-test).

https://doi.org/10.1371/journal.pntd.0007674.g004

XID APerC (30–40%) after 48 h (Fig 4A). At 96 h, the percentage of the death of uninfected BALB/c and XID APerC was similar (about 70%), but a 40 to 50% reduction in the rate of cell death in the infected groups was evident (Fig 4A). In addition, after the infection, the BALB/c and XID APerC behaviors were antagonistic and the rate of apoptosis identified in the infected BALB/c APerC was higher than that observed in XID APerC at both the time intervals (Fig 4B), and infected XID APerC had more necrosis than the other groups (Fig 4C). Similar to our
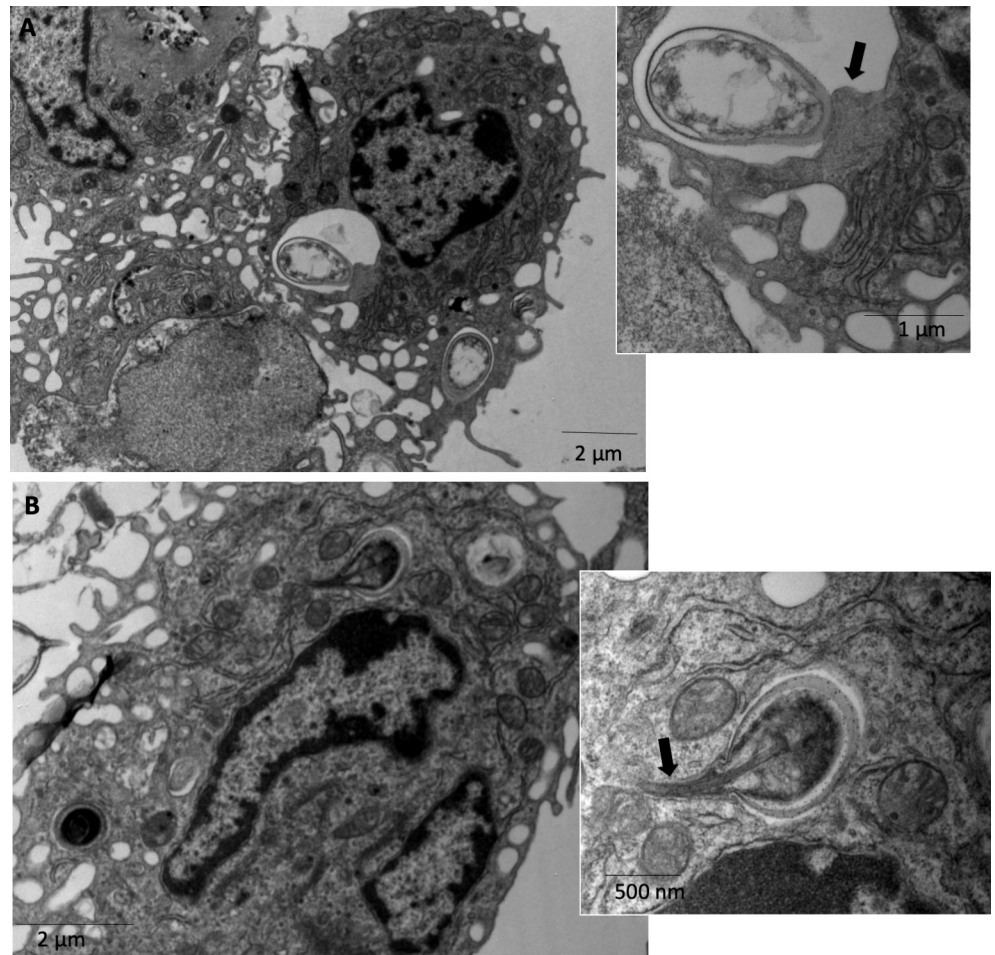
Fig 5. Relations between phagocytes from XID APerC and phagocytized *E. cuniculi* spores after 1 h of infection by ultramicrography. (A) Contact area between the phagocytic vacuole membrane of the macrophages and the internalized spore wall (arrow). (B) Germinated spore with extruded polar tube (arrow) from the phagosome vacuole.

findings, Martin *et al.* [21] reported that *M. tuberculosis*-infected macrophages that die by apoptosis are rapidly engulfed by uninfected macrophages via efferocytosis and this process is responsible for the bactericidal effect associated with apoptosis.

The spores that were internalized by macrophages in XID APerC cultures had a contact area between the phagocytic vacuolar membrane of the cell and the spore wall (Fig 5A and insert), suggesting intimate contact with the phagocytic cells. Furthermore, we observed rarely extrusion of the polar filament by an internalized spore from the phagosome vacuole at 1 h (Fig 5B and insert). The ejection of the polar filament from the phagosome into the cell has been reported in the literature [1], but has not been demonstrated by ultrastructure analysis. This finding suggests an evasion of the microbicidal activity. Therefore, we hypothesize that the absence of B-1 cells could direct the macrophages to M2 profile and favor the dissemination of *E. cuniculi*.

B-1 cells are associated with M1 macrophage profile

To test the influence of B-1 cells in trigger macrophage profile, we evaluated the expression of CD40 and CD206 in macrophages from BALB/c and XID APerC cultures, which may suggest
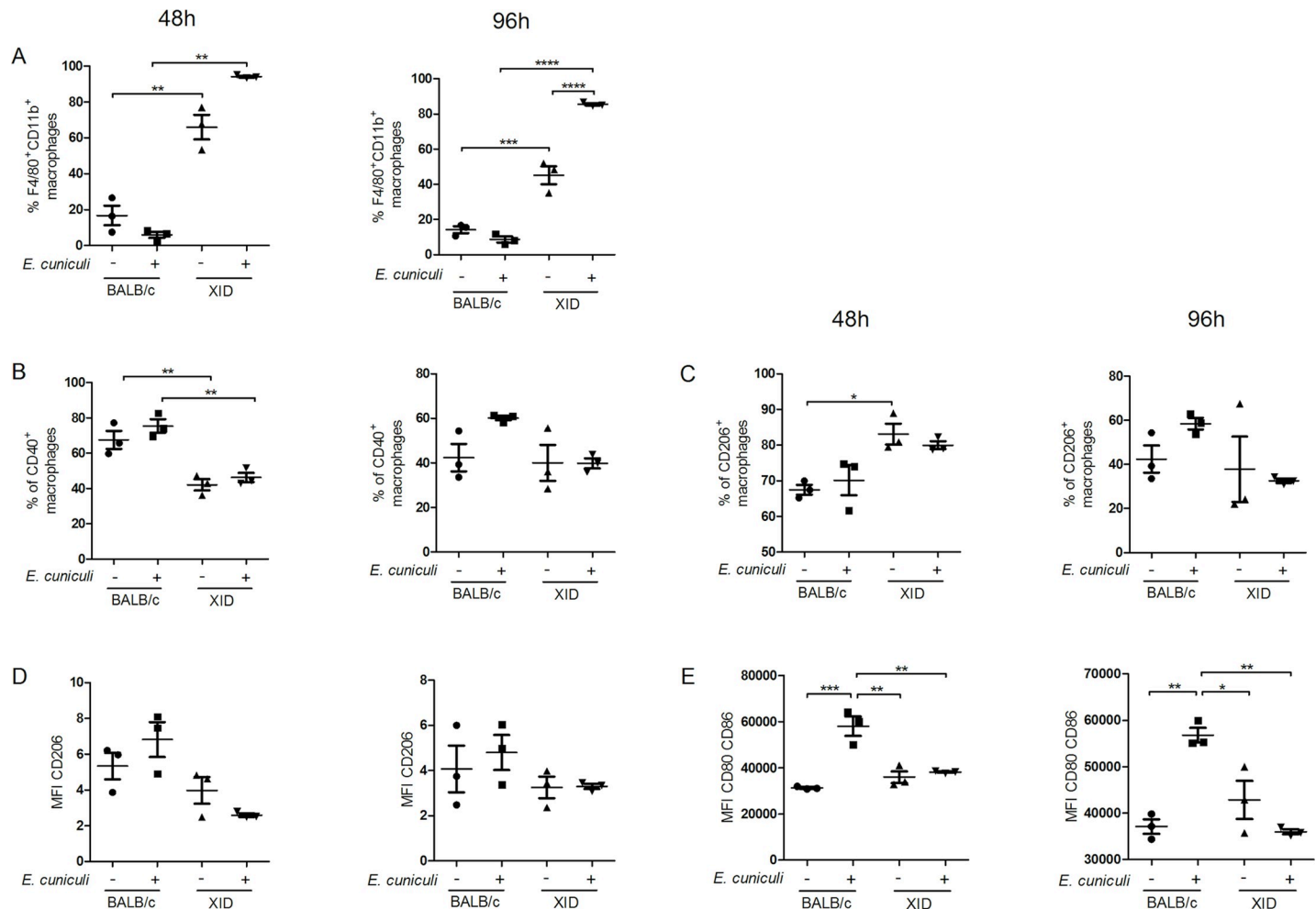
Fig 6. Activation phenotype of macrophages from BALB/c or XID APerC infected with *E. cuniculi* spores. (A) Total percentage of F4/80+CD11b+ macrophages. (B) Proportion of F4/80+CD11b+ macrophages expressing CD40+. (C) Proportion of F4/80+CD11b+ macrophages expressing CD206. (D) Mean fluorescence intensity (MFI) ratio of CD40/CD206 molecules expression on F4/80+CD11b+ macrophages. (E) Mean fluorescence intensity of CD80+ and CD86+ coestimulatory molecules on macrophages. The data are represented as mean ±SEM (* $P < 0.05$, ** $P < 0.01$, *** $P < 0.001$, **** $P < 0.0001$, One way ANOVA with multiple comparisons and Bonferroni post-test).

the classical activation—M1 profile (CD40+high CD206+low) or the alternative activation—M2 profile (CD206+high CD40+low) process. We also analyzed the mean fluorescence intensity of CD80 and CD86 co-stimulatory molecules to measure the activation of these macrophages and aid in the characterization of M1/M2.

The proportion of macrophages in XID APerC (approximately 60%) was significantly higher than that in BALB/c APerC (approximately 20%), regardless of microsporidial infection (Fig 6A). Since the BALB/c culture also contains B-1 cells that adhere together with the macrophages in the first incubation [15,16], this result was expected. After infection, the percentage of macrophages in XID APerC was 80%, which is higher than that observed in uninfected cultures, both at 48 and 96 h (Fig 6A). In BALB/c APerC, no difference was observed in this parameter. At 48 h, approximately 80% of the BALB/c APerC macrophages expressed CD40+ while approximately 40% of XID APerC macrophages expressed CD40+ (Fig 6B). At 96 h, the percentage of these cells decreased to about 60% of CD40+ cells in infected BALB/c AperC and about 40% in infected XID APerC. At 48 h, the CD206+ expression on macrophages was higher in XID APerC than in

BALB/c APerC (Fig 6C). At 96 h, there was no difference between the groups. We also analyzed the mean fluorescence intensity (MFI) ratio of CD40 to CD206 molecules and observed a higher ratio in the infected BALB/c than in XID (Fig 6D), confirming the predominance of CD40 expression in BALB/c APerC. In addition, we observed that infected BALB/c APerC macrophages expressed more CD80 and CD86 costimulatory molecules (Fig 6F) than macrophages from the other groups. These molecules are expressed on the surface of activated macrophages, especially M1 macrophages, which present a higher level of expression. These results together indicate a higher proportion of M1 profile macrophages in BALB/c APerC and M2 profile in XID APerC. The prevalence of *E. cuniculi* infection reinforces these profiles.

E. cuniculi infection modulates macrophage to M2 profile in the absence of B-1 cells

In general, both the pro-inflammatory cytokines (TNF-α and MCP1) and the anti-inflammatory cytokines IL-6 and IL-10 increased 1 hour of infection in the XID infect APerC (Fig 7). While the pro-inflammatory cytokines TNF-α and MCP1 showed no difference in relation to the BALB/c groups, the levels of IL-6 and IL-10 in XID APerC infected were about 4-fold higher than that observed in BALB/c APerC infected. At 30 min, only IL-10 levels were significantly higher in XID than BALB/c, in infected groups. At 48 h, XID APerC infected still had higher levels of cytokines (except TNF-α) than BALB/c APerC infected. At 96 hours, low or undetectable levels of cytokines were observed in all groups.

The activity of B-1 Cell-Derived Phagocyte in *E. cuniculi* infection

It was previously demonstrated that B-1 cells differentiate to acquire a mononuclear phagocyte phenotype following attachment to a substrate *in vitro*, which are named B-1 cell-derived phagocytes (B-1CDPs) [22,23]. It has already been demonstrated that these cells are able to phagocytose various pathogens *in vivo* and *in vitro* [23,24,25,26]. We used B-1 CDP cultures to evaluate the participation of B-1-derived phagocytes in encephalitozoonosis. In B-1 CDP cultures, we observed B-1 CDPs and B-1 cells with preserved characteristics after 1 h and 48 h (Fig 8), indicating that a part of the B-1 cells had become phagocytes. Mussalem *et al*. [27] demonstrated that infection with *Propionibacterium acnes* induced the commitment of B-1 cells to the myeloid lineage and their differentiation into phagocytes. We observed the contact of spores with B-1 cells and pre-B-1-CDPs (Fig 8A). B-1 CDPs with spores of *E. cuniculi* in the process of lysis within phagocytic vacuoles, amorphous material in megasomes (Fig 8B), and intact spores were also visualized in the B-1 CDP cultures (Fig 8C). Other authors also demonstrated the phagocytic and microbicidal ability of peritoneal B-1 cells [28,29]. The ultrastructure of *E. cuniculi* spores was typical of non-germinated mature spores and showed of a thick wall composed of an electron-dense outer layer (exospore), an electron-lucent inner layer (endospore), and a plasma membrane enclosing the cytoplasm (Fig 8C). B-1 cells and pre-B-1 CDP have abundant microvesicles in their membranes (Fig 8D and 8E), indicating exocytosis. Exosomes are nanosized membrane microvesicles that have the capability to communicate intercellularly and to transport cell components [30].

Thus, here we identified two forms of intercellular communication through contact and release of extracellular vesicles (Fig 8A and 8E, respectively). In B-1 CDP cultures, the percentage of dead cells increased at 96 h, as a result of necrosis and apoptosis, regardless of the infection (Fig 9A). Spores outside the cells were identified under light microscopy and low index of phagocytosis was determined after one hour with an increasing trend across the time intervals (Fig 9B). We observed a considerable increase in the pro-inflammatory cytokine TNF-α at 30 min and 1 h in the infected cultures and an increase in MCP1 at 48 and 96 hours (Fig 9C).
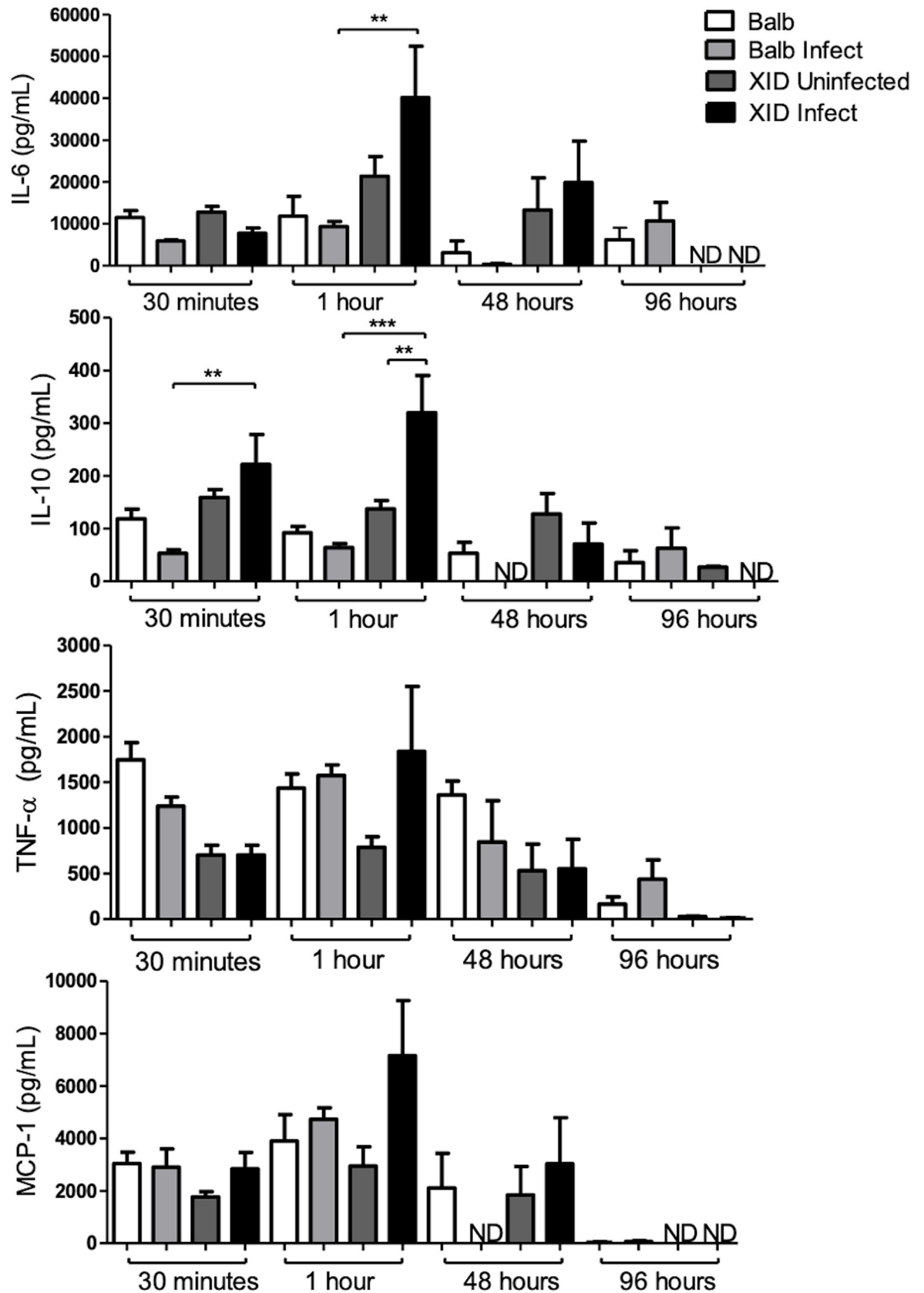
Fig 7. Cytokines levels in the supernatants of BALB/c and XID APerC at 30 minutes, 1 hour, 48 and 96 hours. Data are represented as mean ±SEM (** P <0.01, *** P <0.001and ND = not detected, One-way ANOVA with multiple comparisons and Tukey post-test).

Discussion

The role of B-1 cells in immunity against fungal, protozoan, bacterial, and helminthic infections has been described by us as well as by other researchers. Popi et al. [14] demonstrated that BALB/c mice were more susceptible to experimental infection by *Paracoccidioides brasiliensis* than XID mice, suggesting that B-1 cells may favor infection. This was consistent with other experimentally induced infections, such as *Mycobacterium bovis* bacillus Calmette-Guerin (BCG) [31] and *Trypanosoma cruzi* [32]. B-1 cells secrete IL-10 and use it as an autocrine growth factor. Popi et al. [12] demonstrated *in vitro* that this cytokine decreases the production of nitric oxide and hydrogen peroxide by macrophages, which decreases their phagocytic capacity, compromising the innate immune response and antigenic presentation.

Nevertheless, B-1 cells are critical for the early control of infections with encapsulated bacteria such as *Streptococcus pneumoniae* [33], viruses such as the *Influenza* virus [34], or fungi [35,36]. In line with these studies, our group demonstrated that XID mice were more susceptible to encephalitozoonosis than BALB/c mice, suggesting that the pathogenicity caused by *E. cuniculi* depends on the relationship between the multiplication of parasites and the host immune response [15,16]. In addition, da Costa *et al.* [15] showed that BALB/c mice infected with *E. cuniculi* showed an increase in the number of macrophages and plasma levels of IFN-γ, which was responsible for the activation of macrophages and elimination of the pathogens. Confirming this, here we demonstrated *in vitro* that B-1 cells upregulated the macrophage activity against *E. cuniculi*, characterized by higher phagocytic index and microbicidal capacity, as well as increased macrophage death by apoptosis. The presence of intimate contact between B-1 cells and macrophages suggested communication between these cells and modulation of activity. In addition, B-1 CDP also showed intense phagocytic and microbicidal activities, a fact that may explain the numerical increase of macrophages in BALB/c mice, as previously described by our group [15].

B-1 cells from the peritoneal cavity of mice or cultures of adherent peritoneal cells can be clearly identified on the basis of their distinct morphology and cell surface phenotype. The main morphological characteristic of these cells is the formation of bridges of the nuclear membrane, suggesting a lobular organization of the nucleus. In addition, B-1 cells are characterized by small membrane projections and a large number of ribosomes, a predominance of euchromatin in B-1 cell nuclei, and more condensed chromatin in the nuclear periphery [20]. In this study, we identified B-1 cells by TEM in BALB/c APerC and B-1 CDP cultures. The B-1 CDPs decrease the expression of immunoglobulin M (IgM) but retain the expression of heavy-chain gene-variable VH11 or VH12, an immunoglobulin gene rearrangement that is predominantly expressed by B-1 cells [23]. The maintenance of lymphoid characteristics in B-1 CDPs is the characteristic of a unique type of phagocyte that is not related to monocyte-derived macrophages.

Cell-to-cell communication is required to guarantee proper coordination among different cell types within tissues. Studies have suggested that cells may also communicate by circular membrane fragments called extracellular vesicle that are released from the endosomal compartment as exosomes or shed off from the surface membranes of most cell types [37]. In this study, the identified phagocytic cells of B-1 CDP cultures had abundant extracellular vesicles in their membranes, indicating cell communication. In addition, we observed cells in the process of communicating by cell membrane projections (pseudopodia) or adhered cell-to-cell membrane between different types of cells in BALB/c APerC.
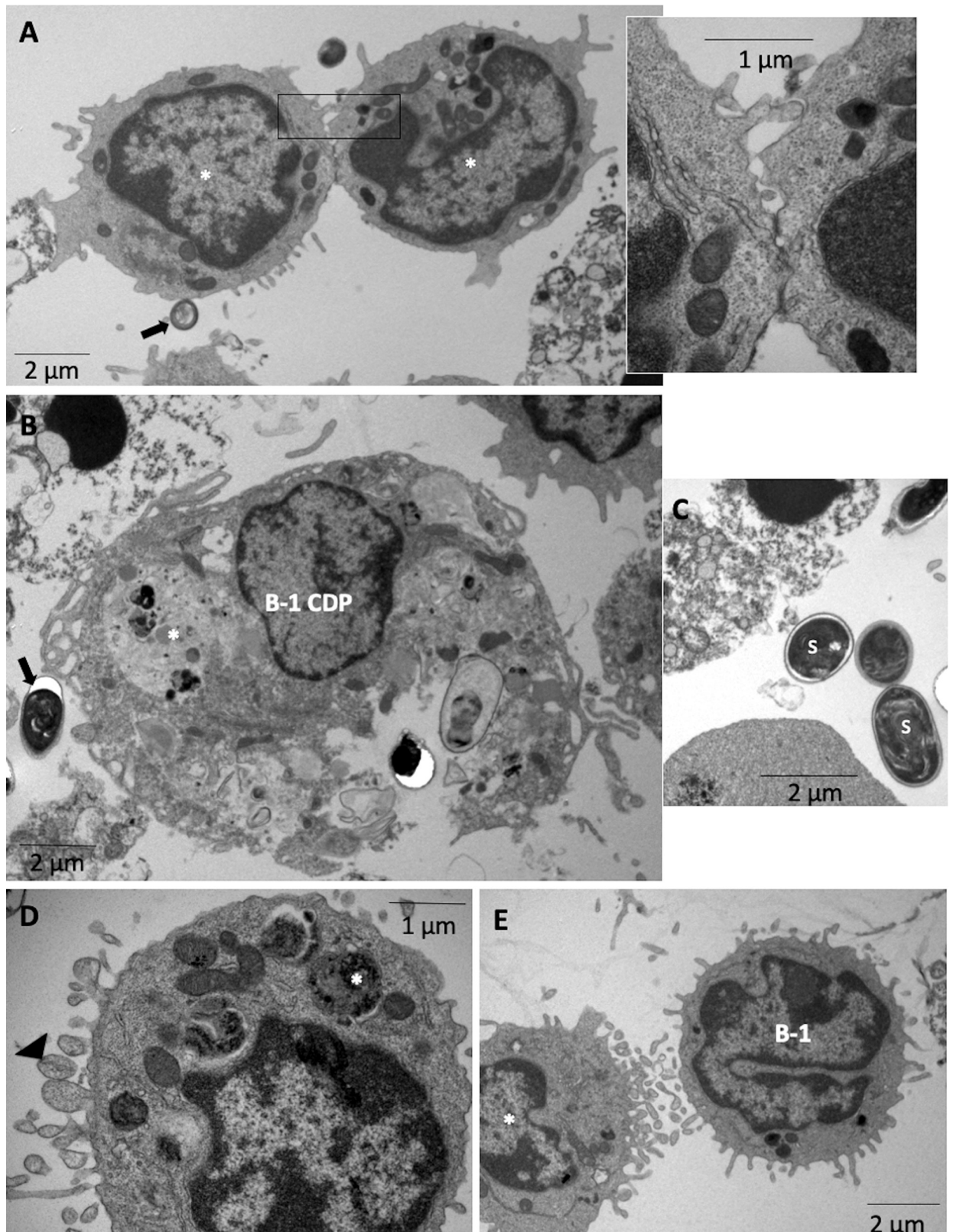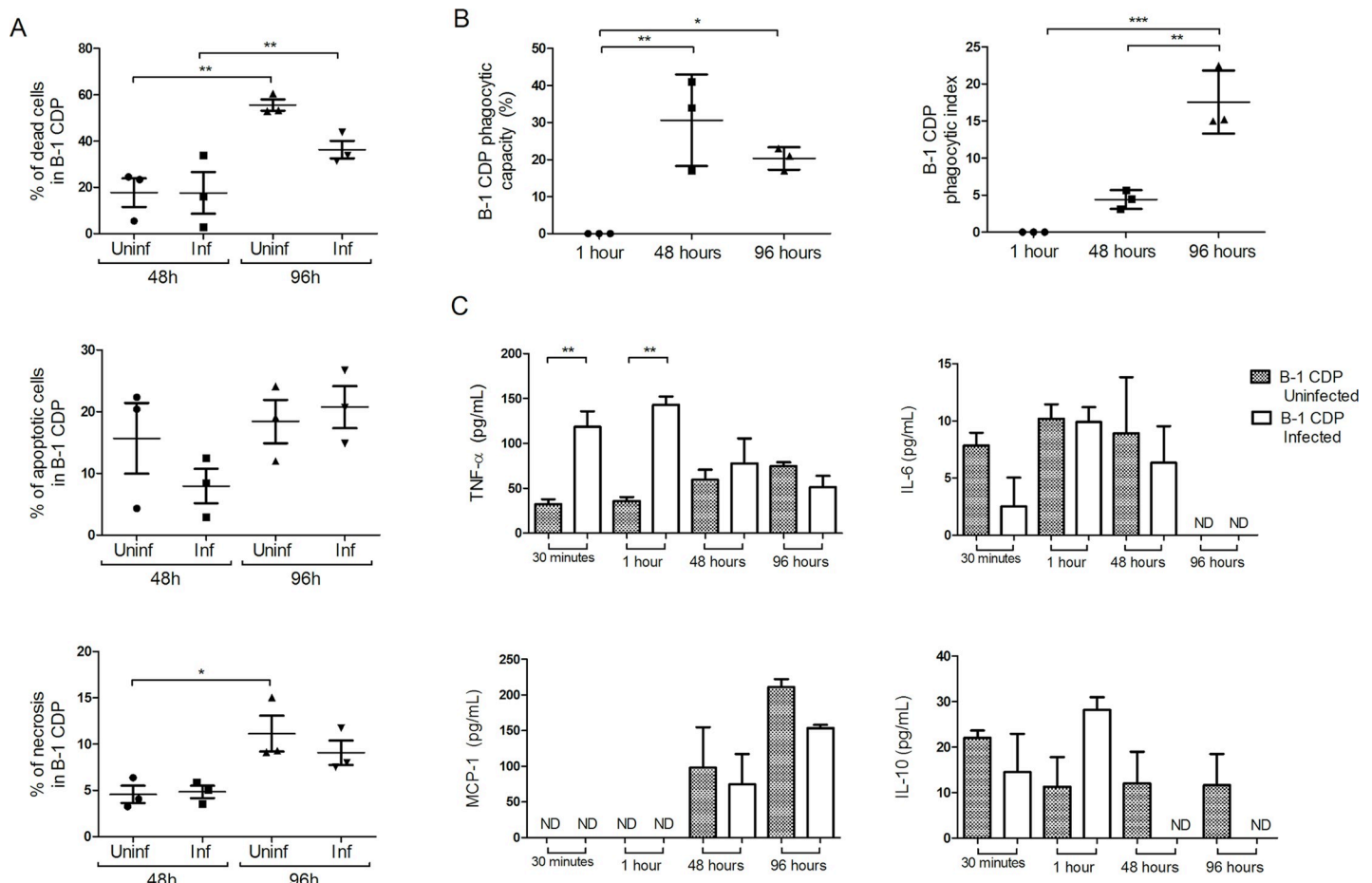
Fig 8. Phagocytic activity of B-1 CDP culture after 1 h and 48 h of infection with *E. cuniculi* by ultramicrography. (A) Pre-B-1 CDP (*) in communication between them and with *E. cuniculi* spores (arrow). Amplified view of the interaction between B-1 cells. (B) B-1 CDP with the

presence of amorphous material inside phagocytic vacuoles (*). (C) Non-germinated spores (s) outside the cells with a thick wall composed of two layers and a plasma membrane. (D) Extracellular vesicles (head arrow) in the membrane of pre-B-1 CDP with the presence of amorphous material (*) inside. (E) Extracellular vesicles in membranes of pre-B-1 CDP (*) and B-1 cell.

The plasticity of macrophages has been demonstrated over the last few years. Depending on the stimulus received by macrophages (pathogens or injured tissue), their receptors trigger a decision to kill (M1) or repair (M2) [38]. The data from transcriptome analysis demonstrated the existence of distinct polarization phenotypes of macrophages associated with specific pathological conditions [39,40]. It is widely accepted that the phenotype of macrophages reflects the immediate microenvironment, wherein other cells can participate in this process. In addition, the role of B-1 cells in the polarization of peritoneal macrophages to an M2 profile in tumor condition was proposed by Wong et al. [41]. In contrast, we demonstrated that macrophages from BALB/c APerC present M1 profile (CD40 ^{high} CD206 ^{low}CD80/86 ^{high}) while macrophages from XID APerC present M2 profile (CD206 ^{high} CD40^{low}CD80/86^{low}). These results may partly explain the susceptibility of XID mice to encephalitozoonosis when compared to BALB/c mice, as previously demonstrated by our group [15]. As demonstrated in this

Fig 9. Necrosis and apoptosis, phagocytic activity and cytokines levels in the supernatants from B-1 CDP cultures. (A) Percentual of death cells, apoptotic cells and necrotic cells in B-1 CDP culture at 48 and 96 h. (B) Phagocytic capacity and phagocytic index in B-1 CDP culture infected with *E. cuniculi* after 1, 48, and 96 h. (C) Cytokines levels after 1, 48, and 96 h post infection with *E. cuniculi*. The data are presented as mean ± SEM (*P < 0.05, ** P < 0.01, *** P <0.001, One way ANOVA with Tukey post-test, ND = not detected).

study, M1 macrophages possess intense phagocytic activity. The presence of megasomes, amorphous material, degenerated spores, and myelin figures within phagocytes in BALB/c APerC confirmed the high microbicidal potential of these macrophages. Furthermore, the expression of CD80 and CD86 produces a second signal necessary for the proliferation and activation of T lymphocytes, a fact that demonstrates the importance of innate response in the production of acquired effective response against microsporidia. APerC infected with *E. cuniculi* showed higher expression of these molecules.

M2 macrophages produce ornithine that promotes proliferation and tissue repair, increasing levels of TGF-β, IL-10, IFN, chitinases, matrix metalloproteinases, scavenger receptors, and have a poor microbicidal function [38,42]. Herein, apart from the M2 profile phenotypically associated with XID APerC macrophages, we observed a lower rate of phagocytosis and delayed microbicidal activity associated with a balance in the production of pro- and anti-inflammatory cytokines, a phenomenon linked with the absence of B-1 cells and *E. cuniculi* infection.

Th2 cytokines have been demonstrated in *E. cuniculi* infection [15,43,44] and an increase in the mRNA for IL-10 was observed in the splenocytes of infected animals [43]. This cytokine has been reported to be involved in the regulation of Th1 immune response against *Toxoplasma gondii* [45] and possibly has a similar role in *E. cuniculi* infection. In an *in vitro* study on cell cultures of human macrophages incubated with *E. cuniculi* spores, an increase in the levels of IL-10 was observed in supernatants of infected cultures. Our findings demonstrated an increase in levels of IL-10 in XID group after 30 minutes and 1 hour of *E. cuniculi* infection, indicating an anti-inflammatory profile. IL-10 is an anti-inflammatory cytokine. During infection it inhibits the activity of Th1 cells, NK cells, and macrophages, all of which are required for optimal pathogen clearance but also contribute to tissue damage [46]. Macrophages are potent antimicrobial effector cells that can participate in both pro-inflammatory (classical M1) and fibrotic (alternatively activated M2) responses [38, 47]. Consequently, it is not surprising that pathogens like *E. cuniculi* have evolved mechanisms to subvert macrophage function or that macrophages are a major source of IL-10 during infection, but in this case it is emphasized that the same occurred in the absence of the B-1 cell in XID group.

IL-6 is a pleiotropic cytokine that mediates several biological functions, including regulation of the immune system by anti-inflammatory and pro-inflammatory production [48]. In a previous study, we demonstrated that diabetes mellitus (DM) increased the susceptibility of C57BL/6 mice to encephalitozoonosis and DM mice infected with *E. cuniculi* showed higher levels of IL-6 than DM-*uninfected* mice, suggesting that DM may also modulate a pro-inflammatory state of the organism [49]. In the current study, we observed an increase in IL-6- in XID APerC after 1 h and 48 h of cultures infection, associated with an increase in the production of IL-10, a fact that suggests an anti-inflammatory effect of IL-6 corroborating the descriptions referring to its pleiotropic behavior, sometimes as a pro-inflammatory cytokine and sometimes as an anti-inflammatory cytokine. In this study, pro-inflammatory cytokine productions also showed an upward trend in Infected XID, suggesting a balance between the production of anti-inflammatory (IL-10 and IL-6) and pro-inflammatory cytokines (TNF and MCP1), however with predominance of the anti-inflammatory profile characteristic of M2 macrophages.

Chemokines are a group of small molecules that regulate cell trafficking of leukocytes. They mainly act on monocytes, lymphocytes, neutrophils, and eosinophils, and play an important role in host defense mechanisms [50]. MCP-1, also known as CCL2, was the first human chemokine to be characterized [51]. This molecule attracts cells of the monocyte lineage, including macrophages, monocytes, and microglia [52]. Mice deficient in MCP-1 were reported to be incapable of effectively recruiting monocytes in response to an inflammatory stimulus,

despite the presence of normal numbers of circulating leukocytes [53]. Chemokine production has been documented to be induced by microsporidian infections in human macrophages. A primary human macrophage culture from peripheral blood mononuclear cells was infected with *E. cuniculi*, revealing the involvement of several chemokines, including MCP-1, in the inflammatory responses [54]. The results showed that in B-1 CDP cultures an increase in MCP1 production occurs at 48 and 96 hours, indicating that the presence of B-1 cells may favor the recruitment of macrophages and the targeting for an M1 phenotype.

The infection process of *E. cuniculi* involves the forced eversion of a coiled hollow polar filament that pierces the host cell membrane, allowing the passage of infectious sporoplasm into the host cell cytoplasm. If a spore is phagocytosed by a host cell, germination will occur and the polar tube can pierce the phagocytic vacuole, delivering the sporoplasm into the host cell cytoplasm [1]. In XID APerC, we observed the extrusion of the polar filaments of intracellular mature spores from the phagolysosomes at 1 h, suggesting that spores may germinate after phagocytosis and escape. This extrusion of the polar tubule has been described in the literature by immunofluorescence [55]. Herein, we showed ultra-micrographic of this process. These findings indicate an intimate relationship between spores and the phagocytic vacuole, suggesting that some XID APerC macrophages have less microbicidal activity. We hypothesize that these macrophages can be polarized to M2 profile in the absence of B-1 cells and promote the maintenance of *E. cuniculi*.

With the results obtained herein, we have demonstrated that B-1 cells modulate the activity of peritoneal macrophages infected with *E. cuniculi* to an M1 profile. Furthermore, part of these cells become B-1 CDPs having microbicidal activity against the pathogen, which explains the lower susceptibility of BALB/c mice to encephalitozoonosis associated with innate immune response.

Methods

Study animals and ethics statement

Inbred specific pathogen free (SPF) BALB/c and BALB/c XID female mice at 6–8 weeks of age were obtained from the animal facility at Centro de Desenvolvimento de Modelos Experimentais (CEDEME), UNIFESP, Brazil. The animals were housed in polypropylene microisolator cages with a 12-hour light-dark cycle, maintained at 21 ±2˚C and >40% humidity, and fed on standard chow and water *ad libitum*.

Ethics statement

All the experimental procedures were performed in accordance with guidelines of Conselho Nacional de Controle de Experimentação Animal (CONCEA) and were approved by the Ethics Committee for Animal Research at Paulista University, under protocol number 385/15.

E. cuniculi spores

Spores of *E. cuniculi* (genotype I) (from Waterborne Inc., New Orleans, LA, USA) that were used in this experiment were previously cultivated in a rabbit kidney cell lineage (RK-13, ATCC CCL-37) in Eagle medium supplemented with 10% of fetal calf serum (FCS) (Cultilab, Campinas, SP, Brazil), pyruvate, nonessential amino acids, and gentamicin at 37˚C in 5% CO_2. The spores were purified by centrifugation and cellular debris was excluded by 50% Percoll (Pharmacia) as described previously [56].

Adherent peritoneal cells (APerC) and B-1 cell-derived phagocyte (B-1 CDP) cultures

The APerC were obtained from the peritoneal cavities (PerC) of BALB/c and B-1 cell-deficient XID mice. PerC were washed using RPMI-1640 medium and 0.5×10^6 cells were dispensed in each well of 24-well plates and incubated at 37˚C in 5% CO_2 for 40 min. Non-adherent cells were discarded and RPMI-1640 supplemented with 10% FCS (R10) was added to the adherent fraction. To obtain B-1 CDP, APerC from BALB/c mice were cultured and the enriched B-1 cells in the floating medium were collected from the third day [57]. Cultures of 0.5×10^6 cells/ well were re-suspended in R10 and re-cultured under the same conditions as described above.

E. cuniculi infection

The culture of BALB/c APerC, XID APerC, and B-1 CDP were infected simultaneously with *E. cuniculi* (1×10^6 spores/mL) in the proportion of two spores per cell (2:1). The cultures were incubated at 37˚C in 5% CO_2 for 30 min, 1h, 48 h, 96 h, and 144 h after infection, following which the supernatants were collected and stored at –80˚C to measure the level of cytokines. The cultures uninfected with *E. cuniculi* were incubated for the same time intervals and used as a group control.

Quantification of cytokines

Cytokines were measured in culture supernatants using Cytometric Bead Array (CBA) Mouse Inflammation Kit (BD Bioscience, San Jose, CA, USA). The kit was used for the simultaneous detection of mouse monocyte chemoattractant protein-1 (MCP-1), interleukin-4 (IL-4), IL-6, IFN-γ, tumor necrosis factor (TNF-α), IL-10, and IL-12p70, according to the manufacturer's instructions. Briefly, the supernatant samples were added to bind to allophycocyanin (APC)-conjugated beads specific for the cytokines listed above and phycoerythrin (PE)-conjugated antibodies. The samples were incubated for 2 h at room temperature in the dark, then measured using FACS Canto II Flow Cytometer, and analyzed by FCAP Array**TM** Software (BD Bioscience), version 3.0. Individual cytokine concentrations (pg/mL) were indicated by the intensity of PE fluorescence and cytokine standard curves.

Flow cytometry of peritoneal cells

Infected and uninfected APerC were detached using a cell scraper and washed with PBS. The cell suspensions were centrifuged and subsequently washed with PBS and re-suspended in 100 μL PBS supplemented with 1% bovine serum albumin (BSA) (PBS-BSA 1%). Each sample was incubated at 4˚C for 20 min with anti-CD16/CD32 to block the Fc II and III receptors. After incubation, the cells were washed, divided into two aliquots, and re-suspended in PBS-BSA 1%. Each sample was then incubated with the following monoclonal antibodies: **1)** fluorescein-isothiocyanate (FITC)-conjugated rat anti-mouse CD80/CD86, 2) PE-Cyanine 5 (PE-Cy5)-conjugated anti-mouse CD40, 3) APC-Cy7-conjugated rat anti-mouse CD11b, and 4) Alexa Fluor 647 rat anti-mouse CD206 (BD-Pharmingen, San Diego, CA, USA) for analysis of the surface markers. The cell pellet was incubated with fluorochrome-conjugated antibodies for 20 min at 4˚C, washed with PBS-BSA 1%, re-suspended in 500 μL of PBS, and analyzed with BD Accuri C6 flow cytometer.

Phagocytic capacity and index

To investigate the phagocytic capacity and index, 10 μL Calcofluor (Sigma-Aldrich, St. Louis, USA) was added per milliliter of the cell cultures to visualize the spores inside the phagocytic

cells. Phagocytic capacity and index were calculated according to the formula: FC = number of phagocytes containing at least one ingested spore/100 phagocytes and FI = total number of phagocytic spores/100 phagocytes containing spores.

Measurement of dead cells

Cell cultures were washed twice with cold PBS and then resuspended in 1x annexin-binding buffer (BD Biosciences) at a concentration of 1×10^6 cells/mL. Thereafter, 100 μL of the solution (1×10^5 cells) was transferred to a 5-mL culture tube, to which 1 μL of PE Annexin V and 1 μL of 7-AAD were added and followed by incubation for 15 min on ice in dark conditions. Subsequently, 400 μL of 1x annexin binding buffer was added to the samples, incubated for 30 min, and all the resultant cell suspensions were analyzed using the BD Accuri C6 flow cytometer.

Analyses using light and transmission electron microscopy

The cell volume of BALB/c APerC, XID APerC, and B-1 CDP cells, cultured as described above, was adjusted to 1×10^7 cells. Each culture was transferred to 25 cm^2 bottles and incubated in the same medium containing 10% FCS (R10) at 37˚C with 5% CO_2 for 40 min. The culture medium was then removed and fresh R10 medium containing *E. cuniculi* spores (2:1) was introduced into the bottles. The cultures were collected after 1 h, 48 h, and 144 h of incubation and fixed using 2% glutaraldehyde in 0.2 M cacodylate buffer (pH 7.2) at 4˚C for 10 h. They were then post-fixed in 1% OsO_4 buffer for 2 h. Semi-thin sections stained with toluidine blue were made for visualization by light microscope, and ultrathin sections were made for TEM analysis.

Statistical analysis

The groups were compared using the two-way analysis of variance (ANOVA) and the significance of the mean difference within and between the groups was evaluated by multiple comparisons using the Bonferroni or Tukey's post-tests. All the experimental data were expressed as mean ± standard error mean, indicated by bars in the figures. *P* values ≤0.05 were considered statistically significant. All the graphs and statistical analyses were made using GraphPad Prism software version 6.0 for Windows (GraphPad Software, San Diego, California, USA).

Supporting information

S1 Fig. Balb and Xid adherent peritoneal cells were cultured in vitro and challenged with *E. cuniculi* for 144 hours. (A) Photomicrography of phagocytic cells with *E. cuniculi* spores inside them (arrow) in APerC XID with 144 h of infection. (B) Ultramicrography of a phagocytic cell with *E. cuniculi* spores in lysis (arrow) in APerC XID after 144 h of infection. (C) Photomicrography of APerC BALB/c in the absence of macrophages and mature spores of *E. cuniculi* outside the cells (arrow) and degenerated lymphocytes (head arrow) after 144 h of infection. (D) Ultramicrography of APerC BALB/c with the absence of macrophages and mature spores of *E. cuniculi* outside the cells (arrow) and degenerated lymphocytes (head arrow) with pyknotic nucleus after 144 h of infection.
(TIFF)

Author Contributions

Conceptualization: Anuska Marcelino Alvares-Saraiva, Mario Mariano, Maria Anete Lallo.

References

1. Ghosh K, Weiss LM. T cell response and persistence of the microsporidia. FEMS Microbiol. Rev. 2012; 36: 748–760. https://doi.org/10.1111/j.1574-6976.2011.00318.x PMID: 22126330

2. Al-Sadi HI, Al-Mahmood SS. Pathology of experimental *Encephalitozoon cuniculi* infection in immuno-competent and immunosuppressed mice in Iraq. Pathol. Res. Int. 2014; 85703: 6.

3. Abu-Akkada SS, Oda SS. Prevention and treatment of *Encephalitozoon cuniculi* infection in immuno-suppressed rabbits with fenbendazole. IJVR. 2016; 17: 98–105 PMID: 27822234

4. Khan IA, Moretto M, Weiss LM. Immune response to *Encephalitozoon cuniculi* infection. Microbes Infect. 2001; 3: 401–405. PMID: 11369277

5. Weidner E, Sibley LD. Phagocytized intracellular microsporidian blocks phagosome acidification and phagosome–lysosome fusion. J. Protozool. 1985; 32: 311–317. https://doi.org/10.1111/j.1550-7408.1985.tb03056.x PMID: 3925132

6. Franzen C, Hartmann P. Salzberger B. Cytokine and nitric oxide responses of monocyte-derived human macrophages to microsporidian spores. Exp. Parasitol. 2005; 109: 1–6. https://doi.org/10.1016/j.exppara.2004.10.001 PMID: 15639133

7. Herzenberg LA. B-1 cells: the lineage question revisited. Immunol. Rev. 2000; 175: 9–22. PMID: 10933587

8. Herzenberg LA, Kantor AB. B-cell lineages exist in the mouse. Immunol. Today. 1993; 14: 79–83. https://doi.org/10.1016/0167-5699(93)90063-Q PMID: 8447936

9. Hardy RR. B-1 B cells: development, selection, natural autoantibody and leukemia. Curr. Opin. Immunol. 2006; 18: 547–555. https://doi.org/10.1016/j.coi.2006.07.010 PMID: 16879952

10. Grönwall C, Vas J, Silverman GJ. Protective roles of natural IgM antibodies. Front Immunol. 2012; 3: 66. https://doi.org/10.3389/fimmu.2012.00066 PMID: 22566947

11. Aziz M, Holodick NE, Tothstein TL, Wang P. The role of B-1 cells in inflammation. Immunol. Res. 2015; 63: 53–166.

12. Popi AF, Lopes JD, Mariano M. Interleukin-10 secreted by B-1 cells modulates the phagocytic activity of murine macrophages in vitro. Immunology. 2004; 113: 348–354. https://doi.org/10.1111/j.1365-2567. 2004.01969.x PMID: 15500621

13. Popi AF, Osugui L, Perez KR, Longo-Maugeri IM, Mariano M. Could a B-1 cell derived phagocyte "be one" of the peritoneal macrophages during LPS-driven inflammation? PLoSOne. 2012; 7: e34570.

14. Popi AF, Godoy LC, Xander P, Lopes JD, Mariano M. B-1 cells facilitate *Paracoccidioides brasiliensis* infection in mice via IL-10 secretion. Microbes Infect. 2008; 10: 817–824. https://doi.org/10.1016/j. micinf.2008.04.012 PMID: 18555722

15. Da Costa LF, Alvares-Saraiva AM, Dell'Armelina Rocha PR, Spadacci-Morena DD, Perez EC, Mariano M, Lallo MA. B-1 cell decreases susceptibility to encephalitozoonosis in mice. Immunobiology. 2017; 222: 218–227. https://doi.org/10.1016/j.imbio.2016.09.018 PMID: 27707513

16. Langanke dos Santos D, Alvares-Saraiva AM, Xavier, JG, Spadacci-Morena DD, Peres GB, Dell'Armelina Rocha PR, Perez EC, Lallo MA. B-1 cells upregulate CD8 T lymphocytes and increase proinflammatory cytokines serum levels in oral encephalitozoonosis. Microbes Infect. 2018; 20: 196–204. https://doi.org/10.1016/j.micinf.2017.11.004 PMID: 29203270

17. Joiner KA. Membrane-protein traffic in pathogen-infected cells. J. Clin. Invest. 1997; 99: 1814–1817 https://doi.org/10.1172/JCI119347 PMID: 9109424

18. Allen LH, Schleisinger LS, Kang B. Virulent strains of *Helicobacter pylori* demonstrate delayed phagocytosis and stimulate homotypic phagosome fusion in macrophages. J. Exp. Med. 2000; 191: 115–128. https://doi.org/10.1084/jem.191.1.115 PMID: 10620610

19. Van Ooij C, Homola E, Kincaid E, Engel J. Fusion of *Chlamydia trachomatis*-containing inclusions is inhibited at low temperatures and requires bacterial protein synthesis. Infect. Immun. 1998; 66: 5364–5371. PMID: 9784545

20. Abrahão TB, Freymuller E, Mortara RA, Lopes JD, Mariano M. Morphological characterization of mouse B-1 cells. Immunobiol. 2003; 208: 401–411.

21. Martin CJ, Booty MG, Rosebrock TR, Nunes-Alves C, Desjardins DM, Keren I, Fortune SM, Remold HG, Behar SM. Efferocytosis is an innate antibacterial mechanism. Cell Host Microbe. 2012; 12: 289–300. https://doi.org/10.1016/j.chom.2012.06.010 PMID: 22980326

22. Almeida SR, Aroeira LS, Frymuller E, Dias MA, Bogsan CS, Lopes JD, Mariano M. Mouse B-1 cell-derived mononuclear phagocyte, a novel cellular component of acute non-specific inflammatory exudate. Int. Immunol. 2001; 13: 1193–1201. https://doi.org/10.1093/intimm/13.9.1193 PMID: 11526100

23. Popi AF, Motta FL, Mortara RA, Schenkman S, Lopes JD, Mariano M. Co- ordinated expression of lymphoid and myeloid specific transcription factors during B-1b cell differentiation into mononuclear phagocytes in vitro. Immunol. 2009; 126: 114–122.

24. Ghosn EE, Russo M, Almeida SR. Nitric oxide- dependent killing of *Cryptococcus neoformans* by B-1-derived mononuclear phagocyte. J. Leukocyte Biology. 2006; 80: 36–44.

25. Novaes e Brito RR, Cortez B, Machado-Santelli G., Xander P., de Lorenzo B., Oliveira H.C., Thies F.G., Kioshima E.S., Maricato JT, Lopes JD, Mariano M. In vitro and in vivo phagocytic ability of mouse B-1 cells. Immunol. Immunogenet. Insights. 2010; 2: 31–39.

26. Gao J, Ma X, Gu W, Fu M, An J, Xing Y, Gao T, Li W, Liu Y. Novel functions of murine B1 cells: Active phagocytic and microbicidal abilities. Eur. J. Immunol. 2012; 42: 982–992. https://doi.org/10.1002/eji. 201141519 PMID: 22531922

27. Mussalem JS, Squaiella-Baptistão CC, Teixeira D, Yendo TM, Thies FG, Popi AF, Mariano M, Longo-Mauregi I. Adjuvant effect of killed Propionibacterium acnes on mouse peritoneal B-1 lymphocytes and their early phagocyte differentiation. PLoSOne. 2012; 7: e33955.

28. Parra D, Rieger AM, Li J, Zhang YA, Randall LM, Hunter CA, Barreda DR, Suney JO. Pivotal advance: peritoneal cavity B-1 B cells have phagocytic and microbicidal capacities and present phagocytosed antigen to CD4^{+} T cells. J. Leukoc. Biol. 2011; 91: 525–536. https://doi.org/10.1189/jlb.0711372 PMID: 22058420

29. Geraldo MM, Costa CR, Barbosa FM, Vivanco BC, Gonzaga WF, Novaes e Brito RR, Popi AF, Lopes JD, Xander P. In vivo and in vitro phagocytosis of *Leishmania* (*Leishmania*) *amazonensis* promastigotes by B-1cells. Parasite Immunol. 2016; 38: 365–376. https://doi.org/10.1111/pim.12324 PMID: 27084328

30. Jones LB, Bell CR, Bibb KE, Gu L, Coats MT, Matthews QL. Pathogens and their effect on exosome biogenesis and composition. Biomedicines. 2018; 6: E79. https://doi.org/10.3390/biomedicines6030079 PMID: 30041409

31. Russo RT, Mariano M. B-1 cell protective role in murine primary *Mycobacterium bovis* bacillus Calmette-Guerin infection. Immunobiol. 2010; 215: 1005–1014.

32. Minoprio P, Coutinho A, Spinella S, Hontebeyrie-Joskowicz M. Xid immunodeficiency imparts increased parasite clearance and resistance to pathology in experimental Chagas' disease. Int. Immunol. 1983; 3: 427–433.

33. Haas KM, Poe JC, Steeber DA, Tedder TF. B-1a and B-1b cells exhibit distinct developmental requirements and have unique functional roles in innate and adaptive immunity to *S. pneumoniae*. Immunity. 2005; 23: 7–18. https://doi.org/10.1016/j.immuni.2005.04.011 PMID: 16039575

34. Choi YS, Baumgarth N. Dual role for B-1a cells in immunity to influenza virus infection. J. Exp. Med. 2008; 205: 3053–3064. https://doi.org/10.1084/jem.20080979 PMID: 19075288

35. Rapaka RR, Ricks DM, Alcorn JF, Chen K, Khader SA, Zheng M, Plevy S, Bengtén E, Kolls JK. Conserved natural IgM antibodies mediate innate and adaptive immunity against the opportunistic fungus *Pneumocystis murina*. J. Exp. Med. 2010; 207: 2907–2919. https://doi.org/10.1084/jem.20100034 PMID: 21149550

36. Szymczak WA, Davis MJ, Lundy SK, Dufaud C, Olszewski M, Pirofski LA. X-linked immunodeficient mice exhibit enhanced susceptibility to *Cryptococcus neoformans* infection. MBio. 2013; 2: 00265–13.

37. Coakley G, Maizels RM, Buck AH. Exosomes and other extracellular vesicles: the new communicators in parasite infections. Trends Parasitol. 2015; 31: 477–489. https://doi.org/10.1016/j.pt.2015.06.009 PMID: 26433251

38. Mills CD. M1 and M2 macrophages: oracles of health and disease. Cri. Rev. Immunol. 2012; 32: 463–488.

39. Noel W, Raes G, Hassanzadeh Ghassabeh G, De Baetselier P, Beschin A. Alternatively activated macrophages during parasite infections. Trends Parasitol. 2004; 20: 126–133. https://doi.org/10.1016/j.pt.2004.01.004 PMID: 15036034

40. Stout RD, Suttles J. Functional plasticity of macrophages: reversible adaptation to changing microenvironments. J. Leukoc. Biol. 2004; 76: 509–513. https://doi.org/10.1189/jlb.0504272 PMID: 15218057

41. Wong SC, Puaux AL, Chittezhath M, Shalova I, Kajiji TS, Wang X, Abastado JP, Lam KP, Biswas SK. Macrophage polarization to a unique phenotype driven by B cells. Eur J Immunol. 2010; 40: 2296–2307. https://doi.org/10.1002/eji.200940288 PMID: 20468007

42. Chávez-Galán L, Olleros ML, Vesin D, Garcia I. Much more than M1 and M2 macrophages, there are also CD169+ and TCR+ macrophages. Front. Immunol. 2015; 6: 263. https://doi.org/10.3389/fimmu.2015.00263 PMID: 26074923

43. Didier ES, Shadduck JA. INF-gamma and LPS induce murine macrophages to kill *Encephalitozoon cuniculi* in vitro. J. Eukaryot. Microbiol. 1994; 41: 34S. PMID: 7804235

44. Khan IA, Moretto M. Role of gamma interferon in cellular immune response against murine *Encephalitozoon cuniculi* infection. Infect. Immun. 1999; 67: 1887–93. PMID: 10085032

45. Gazzinelli RT, Hayashi S, Wysocka M, Carrera L, Kuhn R, Muller W, Roberge F, Trinchieri G, Sher A. Role of IL-12 in the initiation of cell mediated immunity by *Toxoplasma gondii* and its regulation by IL-10 and nitric oxide. J. Eukaryot. Microbiol. 1994; 41: 9S. PMID: 7804285

46. Couper KN, Blount DG, Riley EM. IL-10: The master regulator of immunity to infection. J Immunol. 2008; 180: 5771–5777. https://doi.org/10.4049/jimmunol.180.9.5771 PMID: 18424693

47. Edwards JP, Zhang X, Frauwirth KA, Mosser DM. Biochemical and functional characterization of three activated macrophage populations. J. Leukocyte Biol. 2006; 80: 1298–1307. https://doi.org/10.1189/jlb.0406249 PMID: 16905575

48. Schett G. Physiological effects of modulating the interleukin-6 axis. Rheumatology. 2018; 57: 43–50.

49. Francisco Neto A, Dell'Armelina Rocha PR, Perez EC, Xavier JG, Peres GB, Spadacci-Morena DD, Alvares-Saraiva AM, Lallo MA. Diabetes mellitus increases the susceptibility to encephalitozoonosis in mice. PLoS One. 2017; 12: e0186954. https://doi.org/10.1371/journal.pone.0186954 PMID: 29091912

50. Zlotnik A, Yoshie O, Nomiyama H. The chemokine and chemokine receptor superfamilies and their molecular evolution. Genome Biol. 2006; 7: 243. https://doi.org/10.1186/gb-2006-7-12-243 PMID: 17201934

51. Zlotnik A, Yoshie O. Chemokines: a new classification system and their role in immunity. Immunity. 2000; 12: 121–7. https://doi.org/10.1016/s1074-7613(00)80165-x PMID: 10714678

52. Yoshimura T, Leonard EJ. Human monocyte chemoattractant protein-1: structure and function. Cytokines. 1992; 4: 131–52. PMID: 1472914

53. Lu B, Rutledge BJ, Gu L, Fiorillo J, Lukacs NW, Kunkel SL, North R, Gerald C, Rollins BJ. Abnormalities in monocyte recruitment and cytokine expression in monocyte chemoattractant protein 1-deficient mice. J. Exp. Med. 1998; 187: 601–608. https://doi.org/10.1084/jem.187.4.601 PMID: 9463410

54. Fischer J, West J, Agochukwu N, Suire C, Hale-Donze H. Induction of host chemotactic response by *Encephalitozoon* spp. Infect. Immun. 2007; 75: 1619–1625. https://doi.org/10.1128/IAI.01535-06 PMID: 17178789

55. Franzen C, Muller A, Hartmann P, Salzberger B. Cell invasion and intracellular fate of *Encephalitozoon cuniculi* (Microsporidia). Parasitol. 2005; 130: 285–292.

56. Didier ES, Didier PJ, Friedberg DN. Isolation and characterization of a new microsporidian, *Encephalitozoon hellen* (n. sp.), from three AIDS patient with keratoconjunctivitis. J. Infect. Dis. 1991; 163: 617–621. https://doi.org/10.1093/infdis/163.3.617 PMID: 1995733

57. Alvares-Saraiva AA, Novo MC, de Oliveira VC, Maricato JT, Lopes JD, Popi AF, Mariano M. B-1 cells produce insulin and abrogate experimental streptozotocin-induced diabetes. Eur. J. Immunol. 2015; 45: 1452–1461. https://doi.org/10.1002/eji.201445409 PMID: 25688546